MACEIÓ - ALAGOAS
EBA 15
15° ENCONTRO BRASILEIRO SOBRE ADSORÇÃO
15th Brazilian Meeting about Adsorption

QPVSDM for batch adsorption assuming Langmuir isotherm

Marcelo D.L. Dourado[a], Lucas A. Silva[a], Leandro Vinícius A. Gurgel[b], Marcelo B. Mansur[a,*]

[a] PEMM/UFRJ, Cidade Universitária, Centro de Tecnologia, 21945-970 Rio de Janeiro, RJ, Brazil
[b] DQ/UFOP, Campus Morro do Cruzeiro, Rua Quatro, 786, Bauxita, 35402-136 Ouro Preto, MG, Brazil

Abstract

The Quadratic Pore Volume and Surface Diffusional Model (QPVSDM) incorporates quadratic functions to approximate the intraparticle average concentration profiles of adsorption processes assuming instantaneous reaction, convective external mass transfer, and intraparticle pore and surface diffusions. In this work it was applied to batch operations with local equilibrium given by the Langmuir isotherm, and resulted in an ODE that is simple to solve numerically. Experimental data from real systems reported in the literature were reproduced by the QPVSDM and compared with the classical PVSDM that consists of a PDE system. Both models reached the same equilibrium condition successfully. The QPVSDM was suitable to describe systems with significant surface diffusion effects ($D_{sp} \geq 0.1$). An easy-to-use executable program is available at GitHub platform.

Keywords: adsorption; phenomenological modelling; pore diffusion; surface diffusion; kinetics.

1. Introduction

When applied to describe the dynamic behavior of an isothermal batch adsorption operation in a closed stirred tank assuming spherical adsorbent particles, homogeneous concentration of adsorbate in the external solution, and an instantaneous adsorption rate on the active sites, the classical PVSDM (Pore Volume and Surface Diffusional Model) results in a PDE system comprising the mass balances of adsorbate in the external solution and inside the pores of the adsorbent particles that must be solved numerically. As analytical solutions are restricted to unusual practical situations like infinite bath and linear isotherms, simplified semi-empirical and/or empirical models valid for specific operating conditions (kinetic models of pseudo-first order, pseudo-second order, and intra-particle diffusion) are widely used by experimentalists. To avoid the need for solving a PDE system and develop models that are valid for broad operating conditions, the QPVSDM has been proposed. As it incorporates quadratic functions to approximate the average intraparticle concentration profiles of the process, ODE systems are derived to describe the same phenomenological resistances of the PVSDM (convective external mass transfer and intraparticle pore and surface diffusions), with the advantage of being comparatively simpler to solve numerically.

α	dimensionless Langmuir parameter (= $\rho_p b q_m$)
b	Langmuir parameter (cm³/g)
β	dimensionless Langmuir parameter (= bC_0)
Bi	Biot number (= $k_e R/D_p$)
C_0	external initial conc. (g/cm³)
D_p	effective diffusion coef. (cm²/s)
D_s	surface diffusion coef. (cm²/s)
D_{sp}	dimensionless number (= D_s/D_p)
ε	void fraction of adsorbent (-)
k_e	external mass transfer coef. (cm/s)
m	mass of adsorbent (g)
q	adsorbate mass per adsorbent mass (g/g)
q_m	Langmuir capacity parameter (g/g)
R	radius of adsorbent (cm)
ρ_p	apparent density of adsorbent (g/cm³)
t	time (s)
τ	dimensionless time (= $D_p t/R^2$)
V	volume of the external phase (cm³)
w	dimensionless adsorbate/adsorbent mass ratio (= $\rho_p q/C_0$)
$\bar{w}$	average w
Ω	dimensionless dosage (= $3m/(\rho_p V)$)
y	dimensionless conc. inside pores (= c/C_0)
$\bar{y}$	average y (= $\bar{c}/C_0$)
y^*	dimensionless conc. at external adsorbent's surface (= c^*/C_0)
Y	dimensionless external conc. (= C/C_0)

2. Batch QPVSDM + Langmuir

The QPVSDM is based in two main assumptions:

(1) The adsorption dynamics is experimentally monitored by the adsorbate concentration in the external phase, just as it is unusual to measure the transient concentration profiles inside the particles during operation. As such values are interrelated, it is possible to obtain the external concentration from the average values of the intraparticle functions.

(2) According to the empirical observations by Vermeulen [1], the driving force in diffusive adsorption processes can be approximated by a quadratic concentration profile.

Based on such assumptions, the QPVSDM was applied for batch adsorption with local equilibrium given by the Langmuir isotherm. This can also be done by applying other nonlinear isotherm models, such as Freundlich, Sips, Redlich-Peterson, etc. The model was derived in details elsewhere [2] and presented here solely in dimensionless form:

(i) Adsorbate in the external solution

$$Y(\tau) = 1 - \frac{\Omega}{3}\left[\varepsilon\bar{y}(\tau) + \bar{w}(\tau)\right] \quad (1)$$

(ii) Adsorbate in the pores of the adsorbent

$$\frac{d\bar{y}(\tau)}{d\tau} = \frac{Y(\tau) - \left(\frac{1+\frac{\alpha D_{sp}}{1+\beta\bar{y}(\tau)}}{1+\frac{\alpha D_{sp}}{1+\beta y^*(\tau)}}\right)\bar{y}(\tau)}{\frac{1}{15}\left[\varepsilon + \frac{\alpha}{(1+\beta\bar{y}(\tau))^2}\right]\left(\frac{5}{Bi} + \frac{1}{1+\frac{\alpha D_{sp}}{1+\beta y^*(\tau)}}\right)} \quad (2)$$

(iii) Adsorbed inside the adsorbent (Langmuir)

$$\bar{w}(\tau) = \frac{\alpha\bar{y}(\tau)}{1+\beta\bar{y}(\tau)} \quad (3)$$

where dimensionless concentration on the external surface of the adsorbent y^* is calculated by solving the quadratic equation below for each time interval:

$$\beta\left(\frac{\mathrm{Bi}}{5}+1\right)[y^*(\tau)]^2 + \left[\frac{\mathrm{Bi}}{5} + 1 + \alpha D_{sp} - \beta\left(\frac{\mathrm{Bi}}{5}Y(\tau) + \bar{y}(\tau) + D_{sp}\bar{w}(\tau)\right)\right] y^*(\tau) - \left(\frac{\mathrm{Bi}}{5}Y(\tau) + \bar{y}(\tau) + D_{sp}\bar{w}(\tau)\right) = 0 \quad (4)$$

The model has two transport parameters: the Biot (*Bi)* number represents the ratio of the resistance for pore diffusion to the resistance for convective mass transfer on the external surface of the adsorbent, whereas D_{sp} is the ratio between the surface and pore diffusivities inside the adsorbent particles.

It was solved using the 4th and 5th order of Runge-Kutta method with variable step size. To evaluate the accuracy of the QPVSDM, the PDE system of analogous PVSDM was solved numerically using the method of lines. An easy-to-use executable program is available at https://github.com/marcelo-dourado/adsorption-dynamics.git

3. Applying QPVSDM: Case studies

Batch adsorption data shown in Table 1 were selected as case studies to assess the accuracy of the QPVSDM as compared to the classic PVSDM under the same conditions. In all cases, *Bi* >> 1 reveals that intraparticle mass transfer dominates the adsorption processes for the operating conditions studied. And by comparing pore and surface diffusion resistances, it can be seen that surface diffusion dominates the intraparticle mass transfer for case studies A and B because $\frac{D_s\rho_p q_0}{D_p C_0} > 10$ [6].

Case study	A	B	C
Adsorbate/ adsorbent	Pb/AC*	Levulinic acid/D315**	Mn/bone char
R (cm)	0.060	0.082	0.0317
C_0 (g/cm³)	1×10^{-4}	9.9×10^{-5}	9.98×10^{-5}
ρ_p (g/cm³)	0.48	1.092	1.61
q_0 (g/g)	0.091	0.069	0.018
ε_p	0.743	0.550	0.444
q_m (g/g)	0.1193	0.1476	0.0187
b (cm³/g)	32,000	8,902	674,649
α	1,832.45	1,434.82	20,326.80
β	3.20	0.88	67.33
Ω	1.875×10^{-2}	5.495×10^{-3}	4.65×10^{-3}
k_e (cm/s)	1.08×10^{-3}	1.01×10^{-2}	3.39×10^{-4}
D_p (cm²/s)	8.05×10^{-7}	2.10×10^{-6}	5.60×10^{-7}
D_s (cm²/s)	5.39×10^{-7}	2.73×10^{-7}	1.20×10^{-9}
Bi	80.5	395.0	19.2
D_{sp}	0.67	0.13	0.00214
$\frac{D_s\rho_p q_0}{D_p C_0}$	292.3	98.9	0.6
Reference	[3]	[4]	[5]

* AC = activated carbon; ** Polymeric adsorbent

Case study A: Pb adsorption onto activated carbon

Experimental dimensionless concentration decay curves of Pb confronted with the calculated curves using the models are shown in Figure 1. To enable

a compatible comparison between both models, the intraparticle concentrations obtained with PVSDM were averaged with the radius [2], thus obtaining a concentration profile dependent of time only. Both models reproduced experimental data very well (PVSDM with R^2 = 0.9989 and QPVSDM with R^2 = 0.9996) until reach equilibrium ($Y_{eq} = y_{eq}$ = 0.104 and w_{eq} = 143.2), so they are equivalent for such operating conditions with negligible deviations.

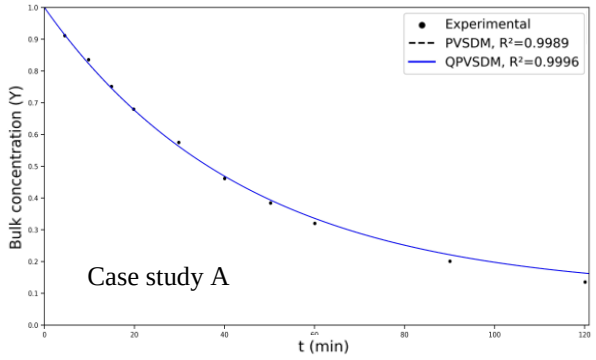

Fig. 1. Dimensionless concentration decay curve.

Case study B: Levulinic acid adsorption onto a polymeric adsorbent

Figure 2 shows the theoretical and experimental dimensionless concentration adsorption decay curves of levulinic acid onto a basic polymeric resin containing a tertiary amine as a functional group. The QPVSDM (R^2 = 0.9808) reproduced data well mainly for longer times, while the PVSDM (R^2 = 0.9954) reproduced it better at shorter times. The equilibrium condition was $Y_{eq} = y_{eq}$ = 0.329 and w_{eq} = 366.1. In terms of the R^2 correlation fit to the experimental data, the QPVSDM is still accurate.

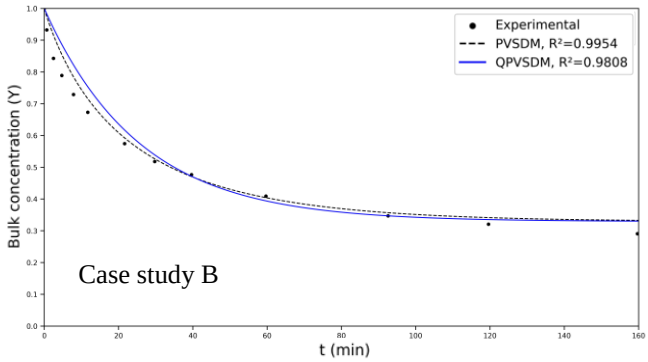

Fig. 2. Dimensionless concentration decay curve.

The QPVSDM/PVSDM deviation ratio between the dimensionless concentration curves calculated by both models is shown in Figure 3. Calculated profiles presented deviation ratios below 10%, excepting the intraparticle concentration profiles at very short times; such behavior is expected due to the inherent quadratic approach used in the QPVSDM (it was found in case study A as well, but below 2%). Despite such a deviation, convergent solutions were also obtained by both simulations.

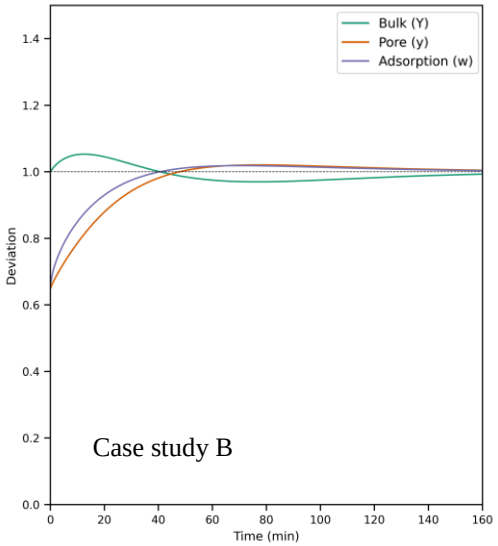

Fig. 3. QPVSDM/PVSDM concentration ratio.

Case study C: Mn adsorption onto bone char

The experimental dimensionless concentration decay curve of Mn onto bone char adsorption is compared with the simulated curves using both models in Figure 4. For the operating conditions, the PVSDM reproduced data well (R^2 = 0.9777), however a suboptimal performance was achieved using the QPVSDM (R^2 = 0.9596); the equilibrium condition was properly calculated ($Y_{eq} = y_{eq}$ = 0.544 and w_{eq} = 293.9).

The comparison between the dimensionless concentration curves calculated using both models is shown in Figure 5. Similarly, as observed in case study B, a larger deviation was found mainly for pore concentration profiles, while the other profile deviations proved to be relatively smaller, within an expected size range. The case study C is characterized by high Bi and low $\frac{D_s \rho_p q_0}{D_p C_0}$ ratio values.

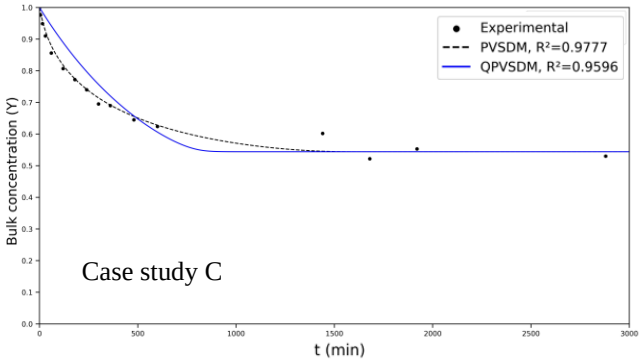

Fig. 4. Dimensionless concentration decay curve.

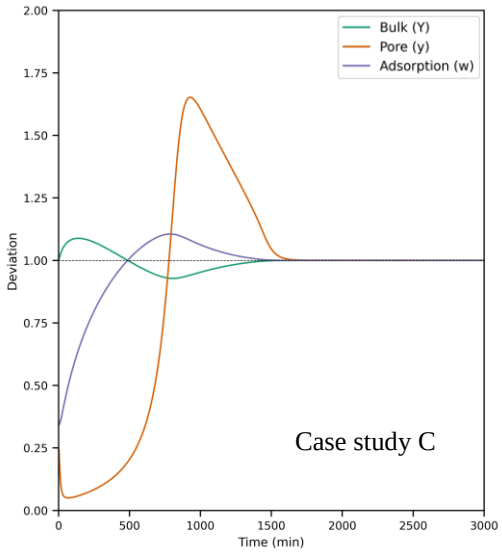

Fig. 5. QPVSDM/PVSDM concentration ratio.

The suboptimal performance of the QPVSDM is due to the low D_{sp} value as illustrated in Figure 6 for the conditions of case study C at distinct D_{sp} values. The discrepancy arises because the term in eq. (2) that accounts for the surface concentration y^* effect vanishes when $D_{sp} \rightarrow 0$. On the contrary, for high D_{sp} values, the discrepancy between models is low; for $D_{sp} \rightarrow 1$ (similar porous and surface diffusion effects), both curves are coincident. In fact, runs using $D_{sp} = 1$ and $0.01 \leq Bi \leq 10{,}000$ resulted in exact same transient profiles for both models. Therefore, based on the case studies evaluated in the present work, the QPVSDM is limited to $D_{sp} \geq 0.1$, with no restriction in terms of Bi values.

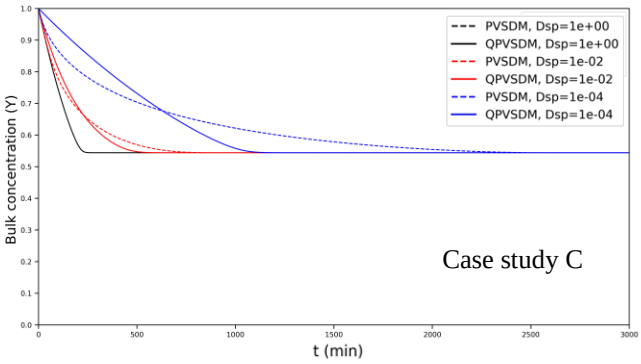

Fig. 7. Dimensionless concentration decay curves at various D_{sp} values (remaining parameters: Table 1).

4. Conclusions

Despite having the same parameters as the PVSDM, the QPVSDM as proposed here consists of a single ODE with an approach function y^* given by eq. (4) easily solved numerically using the Runge-Kutta method. However, it was found to be limited for systems characterized by significant surface diffusion effects ($D_{sp} \geq 0.1$).

Acknowledgements

Thanks to CAPES (822969/2023-00) and CNPq (DTI-A 382348/2022-2, PQ1D 307844/2022-6, and PQ1C 304018/2020-1) for financial support.

References

[1] Vermeulen T. Separation by adsorption methods. Adv Chem Eng 1958;2:147–208.
[2] Dourado MDL, Silva LA, Rodrigues CG, Adarme OFH, Gurgel LVA, Mansur MB. Development of an easy to solve phenomenological model including pore and surface diffusions applied to batch adsorption. Chem Eng Sci 2024;288:119825.
[3] Kavand M, Asasian N, Soleimani M, Kaghazchi T, Bardestani R. Film-pore-[concentration-dependent] surface diffusion model for heavy metal ions adsorption: Single and multi-component systems, Process Safety Env Protection 2017;107:486–497.
[4] Liu B, Yang Y, Ren Q. Parallel pore and surface diffusion of levulinic acid in basic polymeric adsorbents. J Chromatogr A 2006;1132:190–200.
[5] Sicupira DC, Silva TT, Leão VA, Mansur MB. Batch removal of manganese from acid mine drainage using bone char. Braz J Chem Eng 2014;31:195–204.
[6] Inglezakis VJ, Balsamo M, Montagnaro F. Liquid–solid mass transfer in adsorption systems - an overlooked resistance? Ind Eng Chem Res 2020;59:22007–22016.